Ab initio study for adsorption and desorption behavior at step edges of GaN (0001) surface

Toru Akiyama*, Takumi Ohka, Kohji Nakamura, Tomonori Ito

Department of Physics Engineering, Mie University, 1577 Kurima-Machiya, Tsu 514-8507, Japan

ABSTRACT

The adsorption and desorption behavior of adatoms at step edges of GaN(0001) surface is investigated on the basis of *ab initio* calculations. Our calculations of single layer step edges along the [11$\bar{0}$0] direction reveal that the structure of step edge depends on the growth condition. Furthermore, the adsorption behavior of Ga and N adatoms close to the step edges is found to be dependent on these structures. Under moderately Ga-rich and N-rich conditions, Ga adatoms are preferentially incorporated at the step edge with low adsorption energy (-3.7 eV) and the Ehrlich-Schwoebel barrier (ESB) is recognized. On the other hand, the ESB for Ga adatoms is negligibly small under Ga-rich condition. These results suggest that island formation preferentially occurs away from single layer steps under Ga-rich condition, reasonably consistent with experimental results.

1. Introduction

The surface morphology during epitaxial growth is of importance on the efficiency of epitaxially grown quantum devices. It has been experimentally known that smooth GaN layers in the step-flow mode are obtained by both metal-organic vapor phase epitaxy (MOVPE) and Ga-rich plasma-assisted molecular beam epitaxy (PAMBE) [1–5]. It has also been shown that transition between step flow and step bunching during the MOVPE growth of AlN can be controlled by growth parameters such as V/III ratio and substrate off angle [6,7]. Furthermore, hexagonal hillock morphology appears for GaN under N-rich condition in ammonia MBE [4,8] and PAMBE [2,3]. These behaviors are attributed to the kinetic effects: There is an energy barrier located at the step edges called Ehrlich-Schwoebel barrier (ESB), which adatoms need to overcome for diffusing down the step and attach to the lower step edge [9,10]. Since the presence of ESB makes the asymmetry of adsorption-desorption behavior of adatoms, it induces specific self-assembled surface features such as step bunching and meandering [11–13].

Fig. 1 schematically shows the relationship between epitaxial growth and ESB. During the step-flow growth adatoms attach to both the downward or upward step edges as shown in the upper part of Fig. 1(a), while the ESB prevents the incorporation at the downward step edge (Fig. 1(b)). If the ESB is absent, adatoms can be incorporated from both sides of step edges, and step-flow growth occurs when diffusion length λ is much larger than terrace width L. On the other hand, if λ is smaller than L, islands are formed in terrace region, as described

in the bottom part of Fig. 1(a). If the ESB is present, adatoms are incorporated from only lower step, and the nucleation occurs at lower step depending on the diffusion length.

Indeed, the observations of GaN(0001) surfaces in the MBE by scanning tunneling microscopy (STM) clearly demonstrate these kinds of behaviors [14]. The STM images have revealed that islands are formed around terrace and step edges depending on the surface treatment. In particular, triangular-shape islands have been observed in the terrace regions of the surface with 2 monolayer (ML) excess Ga, indicating the absence of ESB in both single and double layer steps. On the other hand, the nucleation close to double layer steps of the surface with 1 ML excess Ga has been found due to the presence of ESB only in double layer steps. Furthermore, the nucleation on the surface without excess Ga layers indicates the presence of ESB for both single and double layer steps. In spite of these experimental findings, the effects of ESB on the growth processes have never been examined from the atom-scale viewpoints.

In our previous study, we have theoretically investigated adsorption and desorption behavior on III-nitride surfaces during the epitaxial growth and revealed characteristic features of adatom kinetics depending on the growth condition such as temperature and pressure [15,16]. Furthermore, we have recently investigated adsorption and desorption behavior on III-nitride surfaces during the epitaxial growth and revealed characteristic features of adatom kinetics depending on the growth condition such as temperature and pressure [15,16]. In this study, we systematically investigate the adsorption and desorption

* Corresponding author.
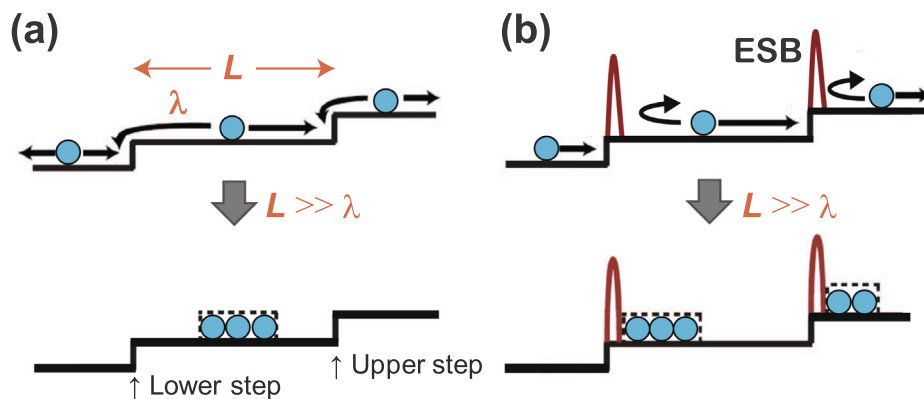 *E-mail address:* akiyama@phen.mie-u.ac.jp (T. Akiyama).

Fig. 1. Schematics of step-flow growth and nucleation on the terrace (a) without and (b) with an Ehrlich-Schwoebel barrier (ESB) at step edges with terrace width L. The nucleation in the terrace occurs when L is much larger than the diffusion length of adatom λ.

behavior of adatoms on stepped GaN(0001) surfaces to clarify the effects of ESB barrier on the growth processes. On the basis of electronic structure calculations within density functional theory (DFT), we examine adsorption and desorption behavior of Ga and N atoms on the surface and discuss its difference between terrace and step edge regions.

2. Methods and models

The total-energy calculations are performed by plane-wave pseudopotential approach using generalized gradient approximation [17] within DFT. We use normconserving pseudopotentials [18] for Ga atoms and ultrasoft pseudopotentials [19] for N atoms. Ga-3d orbitals are adopted by nonlinear core corrections [20]. The calculations using 3d states as valence electrons have found that the structural and electronic properties with partial core corrections are identical to those including 3d electrons as the valence band. The accuracy of the total-energy difference between different structures is estimated to be within 0.1 eV.[21] The conjugate gradient technique [22,23] is utilized for both electronic structure calculations and geometry optimization, and the valence wave functions are expanded by the plane-wave basis set with a cutoff energy of 30.25 Ry. The k-points sampling corresponding to 216-k points in the (1×1) unit cell, which gives enough convergence of total energy (within 0.06 eV) to discuss the relative stability, is employed. The calculated lattice constants for GaN (a = 3.19 Å and c = 5.25 Å) in wurtzite structure agree well with the experimental values [24] as well as previous calculations [25]. Computations have been performed using extended Tokyo *Ab initio* Program Package (xTAPP) [26,27].

In this study, we consider stepped surface models for the MBE growth. Fig. 2 depicts the slab models to clarify the adsorption and desorption behavior of Ga and N adatoms on stepped GaN(0001) surface. We consider only single layer steps, and these are simulated by vicinal (2×9) slab models consisting on six bilayer GaN terminated by artificial H atoms [28]. The surfaces consist of two (2×4) terrace regions and two single layer steps, resulting in periodic (2×9) vicinal slab models. Details of the unit cell of vicinal (2×9) slab models are described in Fig. 3. Owing to the presence of step edges, the (2×9) unit cell is necessary to simulate the vicinal surface consisting of two (2×4) and two single layer step edges. It should be noted that two different atomic configurations labeled as Step A and Step B in Figs. 2(a) and 3(b) appear at the step edge due to the stacking sequence (AB stacking) of wurtzite structure along the [0001] direction. The slab models contain 12 Å vacuum region to eliminate the interaction between adjacent slabs, and various atomic configurations and structures are considered. These models are constructed on the basis of electron counting (EC) rule [29] and previously reported reconstructions on GaN(0001) surface during the MBE growth [15,16,30–32]. Terrace regions are constructed by multiplying the (2×2) periodicity to satisfy the EC rule

[29]. The surface with N atoms (N_{ad}) shown in Fig. 2(a) is constructed based on the (2×2) surface with N adatom under N-rich condition and that with Ga atoms (G_{ad}) shown in Fig. 2(b) on the (2×2) surface with Ga adatom under moderately Ga-rich condition. Furthermore, the surfaces with 1 and 2 ML excess Ga (Figs. 2(c) and 2(d), respectively) are taken into account for the reconstructions under Ga-rich condition. In order to determine the stable step edge structures, we evaluate the formation energy of step edge $E_{\text{form}}(\mu_{\text{Ga}})$ as a function of Ga chemical potential μ_{Ga}. The formation energy is given by

$$E_{\text{form}}(\mu_{\text{Ga}}) = E_{\text{tot}} - E_{\text{ref}} - (n_{\text{Ga}} - n_{\text{N}})\mu_{\text{Ga}} - n_{\text{N}}E_{\text{GaN}}, \qquad (1)$$

where E_{tot} and E_{ref} are the total energy of the slab under consideration and that of the reference (*i.e.*, ideal stepped surface), respectively. n_{Ga} and n_{N} are the number of excess or deficit Ga and N atoms with respect to the reference, respectively, and E_{GaN} is the total energy per formula unit of bulk GaN. The relationship between μ_{Ga} and the chemical potential of N (μ_{N}) expressed as $\mu_{\text{Ga}} + \mu_{\text{N}} = E_{\text{GaN}}$, is used as the equilibrium condition.

The adsorption behavior along the [1$\bar{1}$00] direction on the vicinal (2×9) surface is obtained from the calculated adsorption energies at various positions. To elucidate adsorption and diffusion of adatoms on the surface, the potential-energy profiles are calculated by fixing the adatom in the [1$\bar{1}$00] direction at various positions and allowing the relaxation of adatom normal to the [1$\bar{1}$00] direction, while the other atoms are fully relaxed. The initial positions of the adatom are determined on the basis of the results of adatoms on planar GaN(0001) and AlN(0001) surfaces [33–36]. We use 27 inequivalent linear positions to sample the unit cell. The adsorption energy of Ga and N adatoms E_{ad} is obtained by the total energy difference between the surfaces with and without adatom. In addition to the calculations for potential-energy profiles on the vicinal (2×9) surfaces, we calculate the potential-energies on flat (2×2) surfaces to clarify the effect of step edges on the adsorption and desorption behavior of Ga and N adatoms. Details of calculation procedure are described elsewhere [35].

3. Results and discussion

Fig. 4 shows the calculated formation energy of vicinal (2×9) surfaces as a function of μ_{Ga}. It is found that the stable structure depends on the Ga chemical potential and three types of structures can be mainly stabilized during the MBE. The surface with Ga atoms shown in Fig. 2(b) is stabilized under moderate Ga-rich and N-rich conditions (for $\mu_{\text{Ga}} \leqslant -1.04$ eV), while that with 1 ML excess Ga shown in Fig. 2(c) is favorable under Ga-rich condition. Furthermore, the surface with 2 ML excess Ga is stabilized close to Ga-rich limit for $\mu_{\text{Ga}} \geqslant -0.03$ eV. Since the surface with N atoms is stabilized under N-rich limit, it is reasonable to assign three types of reconstructions for the MBE. The trend of stable structures is therefore similar to the trend of planar GaN(0001) surface
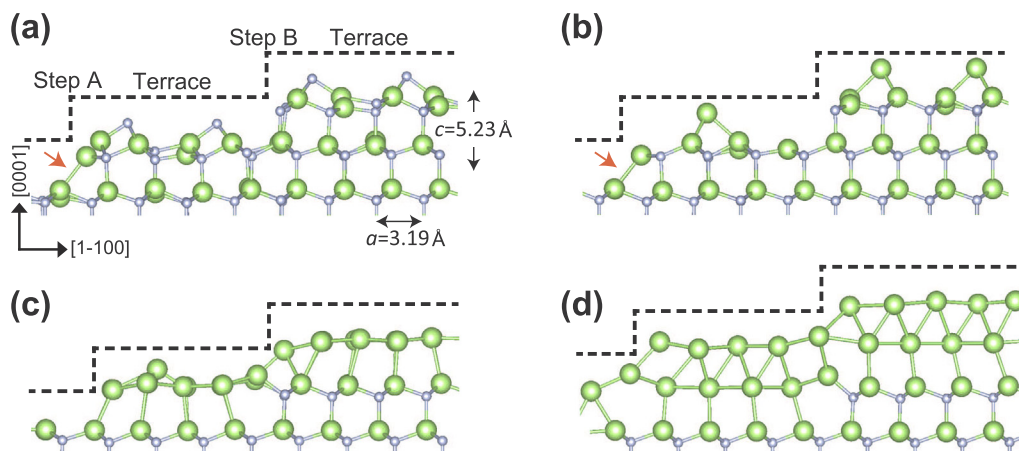
Fig. 2. Geometries of vicinal (2×9) slab models for stepped GaN(0001) surfaces with (a) N atoms (N_{ad}), (b) Ga atoms (Ga_{ad}), (c) 1 ML excess Ga, and (d) 2 ML excess Ga considered in this study. Green and purple circles denote Ga and N atoms, respectively. Dashed stepwise lines indicate the step and terrace regions along the [11$\bar{0}$0] direction. Ga-Ga dimers formed at one of step edges are indicated by arrows. Note that periodic boundary conditions is imposed along the [11$\bar{0}$0] direction and two single layer steps whose height is 2.63 Å are included in the unit cell.

[30]. It should be noted that different atomic configurations appear at the step edges due to the symmetry of wurtzite structure. Ga-Ga dimers are formed at the lower step edge of N_{ad} and Ga_{ad} shown in Figs. 2(a) and 2(b), respectively, to reduce the number of dangling bonds. Indeed, the difference in atomic configurations at the step edge is crucial for the adsorption behavior of adatoms, which is discussed later.

On the basis of step edge structures obtained by the formation energies shown in Fig. 4, the adsorption and desorption of Ga and N is examined. We note that the potential-energy profile near Step A is different from that near Step B due to the inequivalent step edges. Fig. 5 shows the positions of Ga and N atoms and their potential-energy profiles along the [11$\bar{0}$0] direction on the stepped surface with Ga
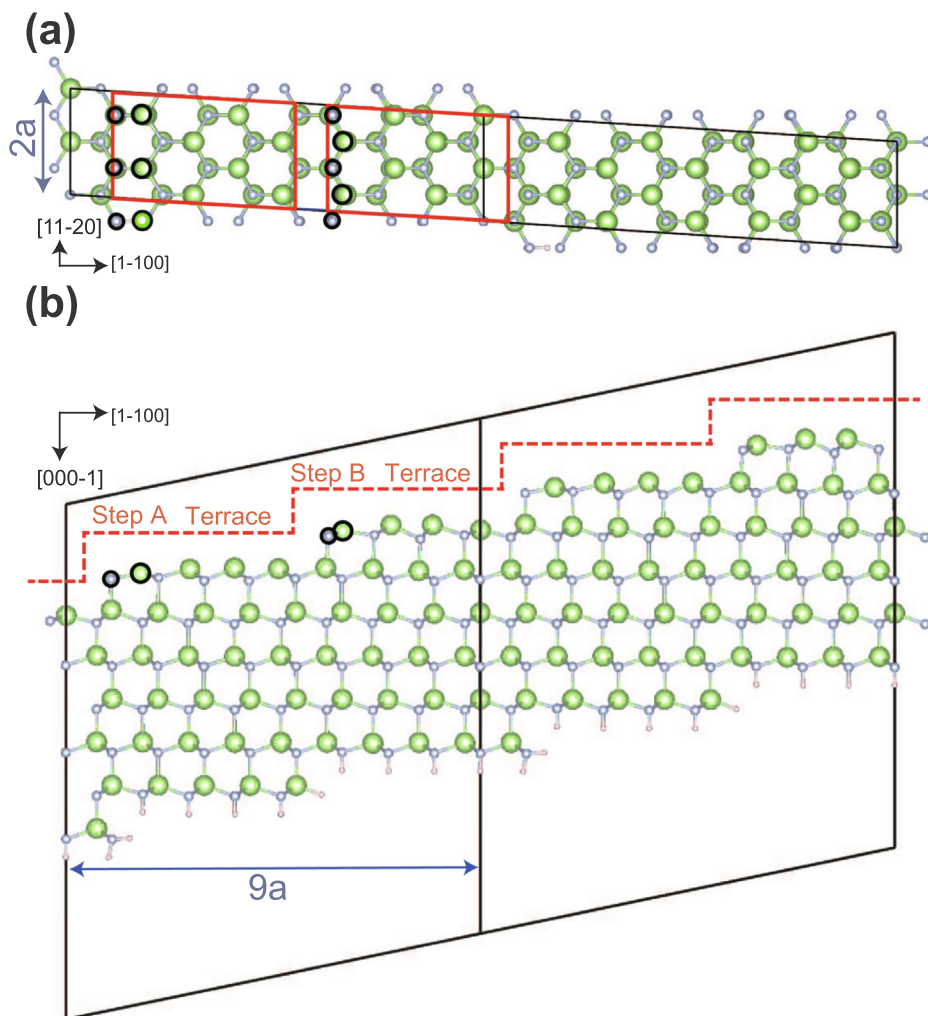

Fig. 3. (a) Top and (b) side views of vicinal slab model for ideal GaN(0001) surface. Green, purple, and pink circles denote Ga, N and artificial H atoms, respectively. Black circles represent the atoms of step edges. Black rectangles represent the unit cells. The unit cell is multiplied along the [11$\bar{0}$0] direction for visual understanding. Dashed stepwise lines in side view indicate step and terrace regions along the [11$\bar{0}$0] direction. The surface consists of two (2×4) terrace regions (red rectangles) and two single layer steps, which results in (2×9) vicinal slab model. (For interpretation of the references to colour in this figure legend, the reader is referred to the web version of this article.)
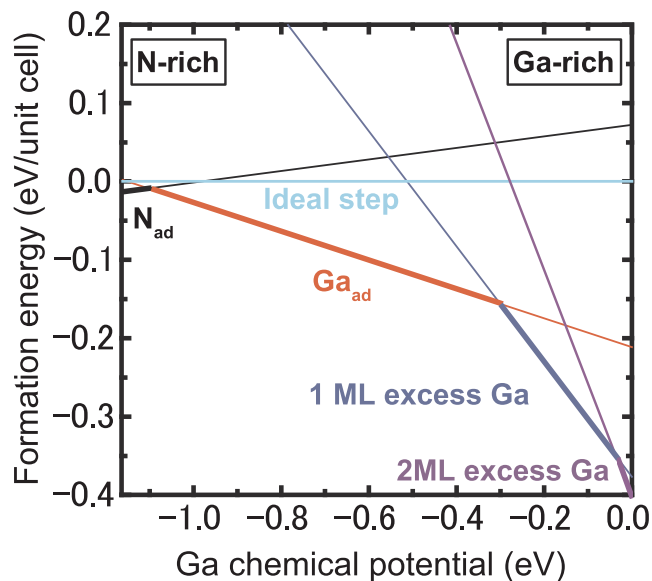
Fig. 4. Calculated formation energies of various step-edge structures on GaN (0001) surface as a function of Ga chemical potential μ_{Ga}. The origin of μ_{Ga} is set to the energy of bulk Ga. Geometries of step edges are shown in Fig. 2.

atoms shown in Fig. 2(b). As seen in the potential-energy profile of the Ga adatom shown in Fig. 5(a), the most stable adsorption site is located close to Step B with $E_{ad} = -3.71$ eV. This value is much lower than the adsorption energy on the flat (0001) surface, indicating that the Ga adatom is easily incorporated in the step edge. Another important feature in the potential-energy profile is found in the step edge consisting of Ga-Ga dimer. The adsorption energy is much higher than that in the terrace regions. As a result, there is a large energy barrier to overcome for diffusing down the step, which corresponds to the ESB.

The values of ESB (E_{ESB}) estimated from the difference in barriers for step attachment between the upper and lower terraces are thus 1.0 eV for Step A and -1.2 eV for Step B. By comparing the adsorption energy with gas-phase chemical potential of Ga atom using the partition function of translational motion for ideal gas (-3.5 eV)[37] at 1000 K with low pressure condition, it is thus suggested that Ga adatoms near the step edge with Ga-Ga dimer easily desorb from the surface in addition to the inhibition of Ga diffusion. Another important quantity for step flow growth in MBE is the step attachment energy, which is the energy difference between the adatom at the step edge and that at the neighboring terrace. The calculated attachment energy is 1.27 (-0.78) eV for Step A (Setp B), implying that the attachment of Ga adatoms is preferable only at Step B.

In contrast, as for the adsorption of N adatom shown in Fig. 5(b), there are large energy differences depending on the position of adsorption sites. The most stable adsorption site for the N adatom is located in the terrace region rather than step edges, and the value (-5.04 eV) of E_{ad} is much lower than that of Ga adatom. Due to the large energy difference more than 2 eV between the most stable site and the other site, it is expected that the N adatom hardly diffuses and is trapped in the stable sites. Although the reduction of diffusion energy barrier of N adatom in the presence of a nearby Ga adatom on the flat (0001) surface has been proposed [36], the effect of Ga preadsorbed atoms on the diffusion of N adatom is hardly found near the step edges. The calculated attachment energies for the N adatom are 0.75 and 0.57 eV for Step A and Step B, respectively.

Fig. 6 shows the positions of Ga and N atoms and their potential-energy profiles along the [11$\bar{0}$0] direction on the stepped surface with 1 ML excess Ga shown in Fig. 2(c). The potential-energy profile of the Ga adatom shown in Fig. 6(a) reveals that the most stable adsorption site is located close to the step edge. However, the adsorption energy near Step B ($E_{ad} = -2.68$ eV) is close to those in the other positions. The small energy difference in the adsorption energy is due to the formation of Ga-Ga bonds between the adatom and topmost atoms
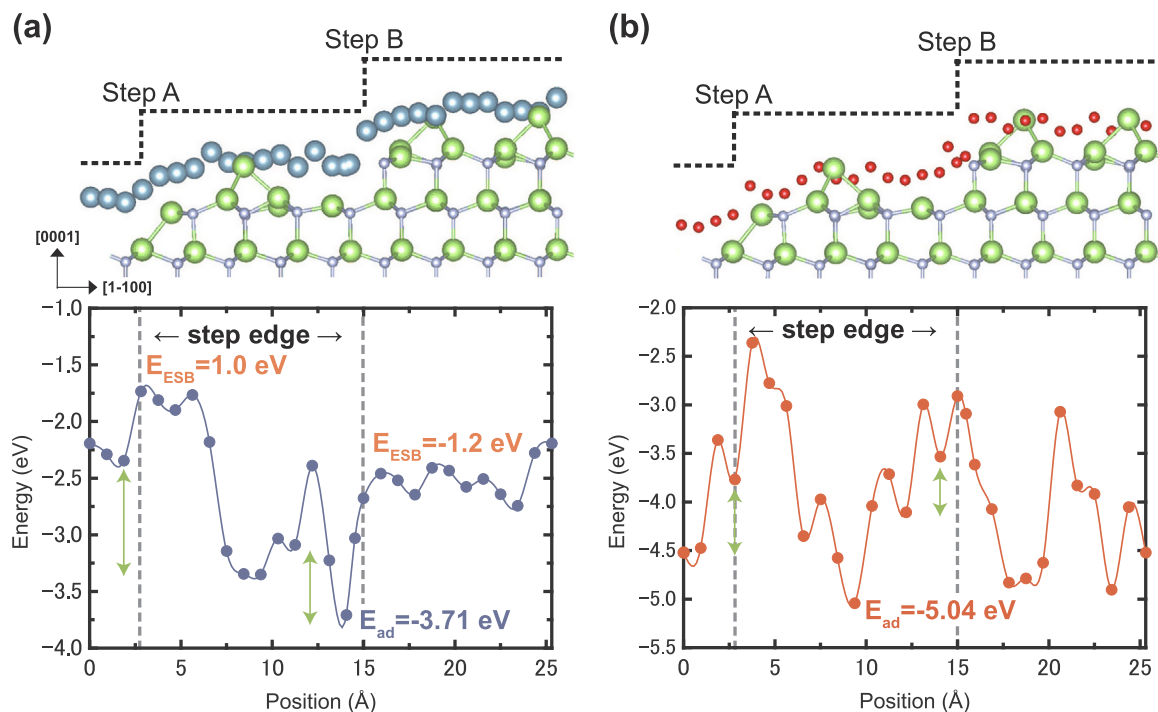

Fig. 5. One-to-one correspondence between the position of the adatom and its adsorption energies along the [11$\bar{0}$0] direction for (a) Ga and (b) N near the step edges on GaN(0001) surface with preadsorbed Ga atoms shown in Fig. 2(b). Side views of Ga and N adatoms at each position on the stepped GaN(0001) surface are shown by blue and read circles, respectively. Green and purple circles denote Ga and N atoms of stepped surface, respectively. Calculated adsorption energies of Ga and N atoms at the most stable site are also shown. Attachment energy of the adatom for each step edge is represented by green arrow. (For interpretation of the references to colour in this figure legend, the reader is referred to the web version of this article.)
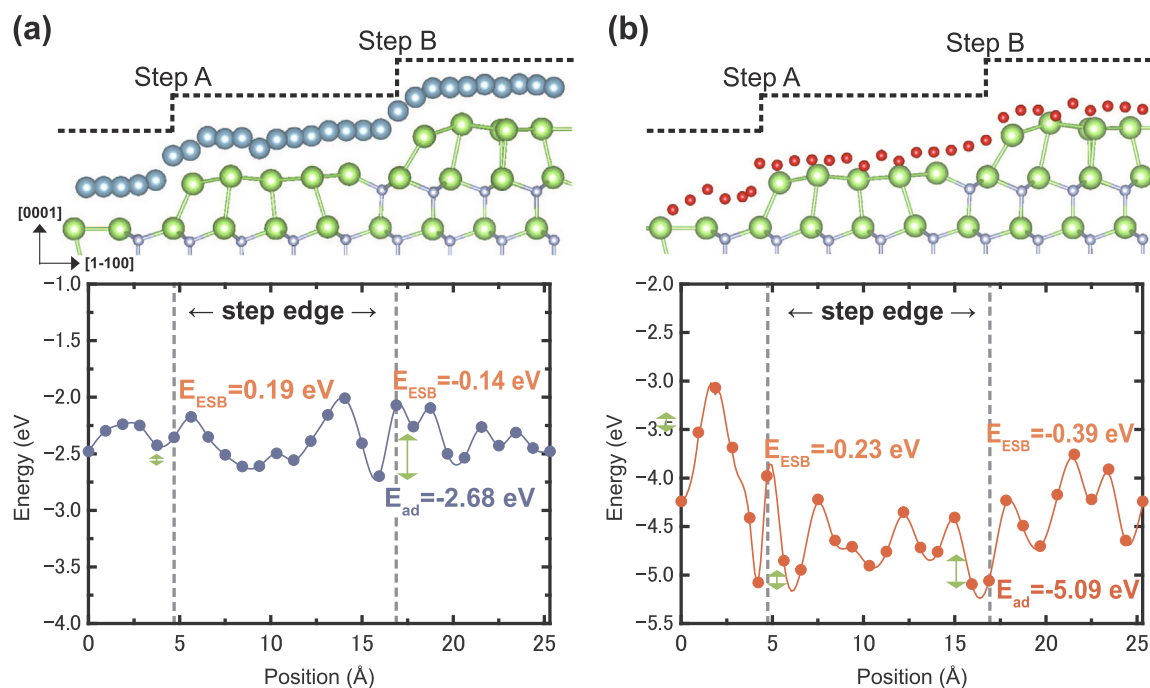
Fig. 6. One-to-one correspondence between the position of the adatom and its adsorption energies along the [11̄00] direction for (a) Ga and (b) N near the step edges on GaN(0001) surface with 1 ML excess Ga shown in Fig. 2(c). Notations of atoms are same as those in Fig. 5. Calculated adsorption energies of Ga and N atoms at the most stable site are also shown. Attachment energy of the adatom for each step edge is represented by green arrow. (For interpretation of the references to colour in this figure legend, the reader is referred to the web version of this article.)
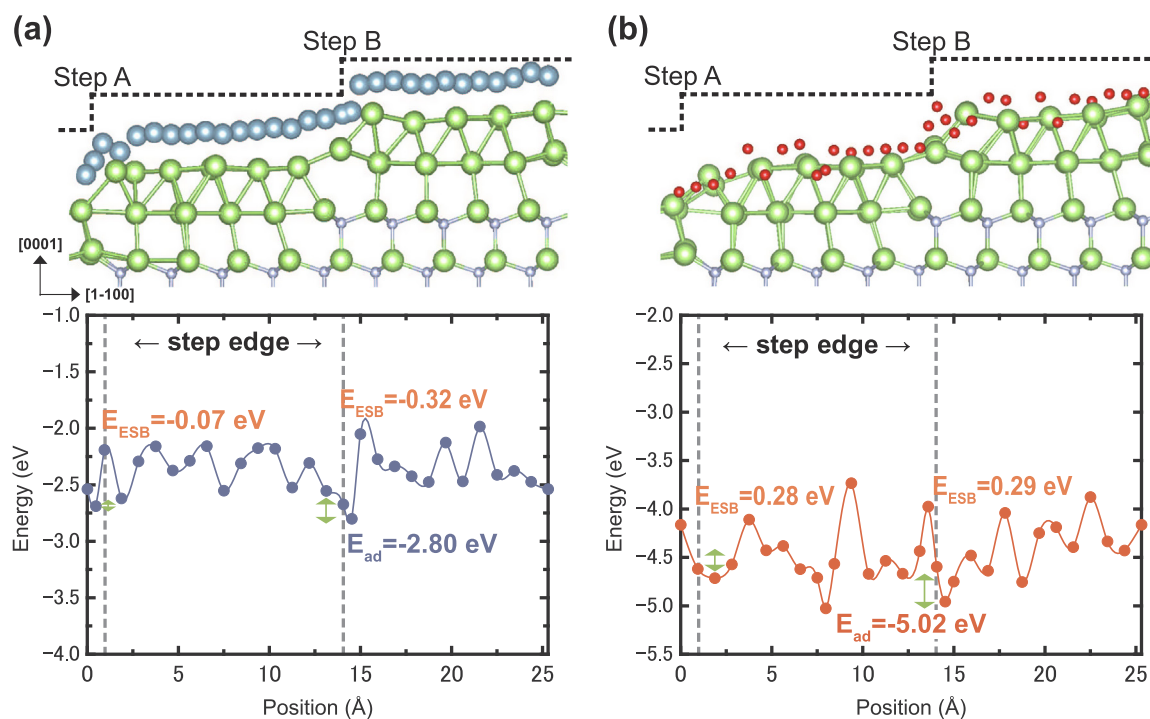

Fig. 7. One-to-one correspondence between the position of the adatom and its adsorption energies along the [11̄00] direction for (a) Ga and (b) N near the step edges on GaN(0001) surface with 2 ML excess Ga shown in Fig. 2(d). Notations of atoms are same as those in Fig. 5. Calculated adsorption energies of Ga and N atoms at the most stable site are also shown. Attachment energy of the adatom for each step edge is represented by green arrow.

irrespective of the position of Ga adatom. Furthermore, the energy barrier for the Ga adatom around the step edge is at most 0.67 eV. The calculated values of ESB are 0.19 eV for Step A and −0.14 eV for Step B, implying that there is few specific energy barrier to overcome for diffusing up and down the step. The calculated attachment energies for the Ga adatom are 0.05 and −0.42 eV for Step A and Step B,

respectively.

The adsorption of N adatom shown in Fig. 6(b) is rather different from that of Ga adatom. In the case of surface with 1 ML excess Ga, the most stable adsorption site for the N adatom is located close to Step B with $E_{ad} = -5.09$ eV, but the value is only 0.2 eV lower than the other positions. The small energy difference in the adsorption energy implies
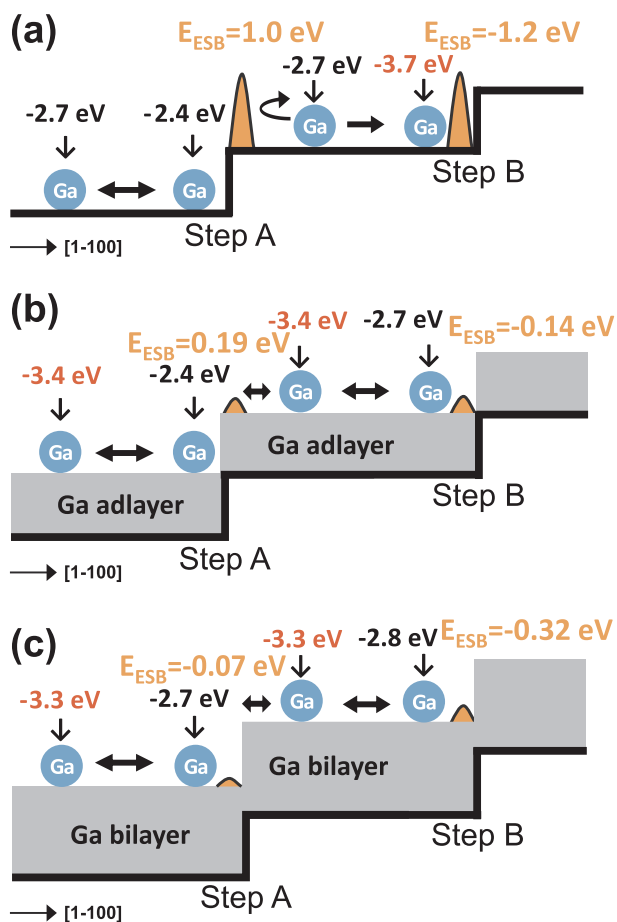
(a)

$E_{ESB}=1.0$ eV $E_{ESB}=-1.2$ eV

-2.7 eV -3.7 eV

-2.7 eV -2.4 eV

Ga ⟷ Ga   Ga → Ga

Step B

[1-100]   Step A

(b)

-3.4 eV -2.7 eV $E_{ESB}=-0.14$ eV

$E_{ESB}=0.19$ eV

-3.4 eV -2.4 eV

Ga ⟷ Ga   Ga ⟷ Ga

Ga adlayer

Ga adlayer   Step B

[1-100]   Step A

(c)

-3.3 eV -2.8 eV $E_{ESB}=-0.32$ eV

$E_{ESB}=-0.07$ eV

-3.3 eV -2.7 eV

Ga ⟷ Ga   Ga ⟷ Ga

Ga bilayer

Ga bilayer   Step B

[1-100]   Step A

Fig. 8. Schematics of adsorption and desorption behavior of Ga adatoms near the single step edges of reconstructed GaN(0001) surfaces with (a) Ga atoms, (b) 1 ML excess Ga, and (c) 2 ML excess Ga obtained from Figs. 5(a), 6(a), and 7(a). The adsorption energies at terraces are obtained from the (2×2) flat slab models. Stepwise lines indicate the step and terrace regions along the [1 1 $\bar{0}$ 0] direction. Shaded area denote Ga adlayer and Ga bilayer.

that the adsorption of N adatoms occurs not only near the step edge but also in the terrace region. In addition, there is a large energy barrier to overcome for diffusing upward the step, which corresponds to inverse ESB. This is because the N adatom forms a single Ga-N bond resulting in a high adsorption energy. The values of E_{ESB} estimated from the difference in barriers for step attachment between the upper and lower terraces are -0.23 eV for Step A and -0.39 eV for Step B. However, the N adatom is also stabilized when it is located underneath the Ga layer by forming Ga-N bonds: The adsorption energy for this configuration is -5.94 eV. Therefore, the N adatom tends to diffuse into the bulk and is trapped in the adsorption sites underneath the Ga layer. The calculated attachment energies for the N adatom are -0.13 and -0.30 eV for Step A and Step B, respectively. For the N adatom on planner GaN(0001) surface under Ga-rich condition, the diffusion within subsurface has been verified [38]. This indicates that the diffusion of N adatom within subsurface could occur even at the step edges. Further calculations might be necessary for detailed understanding of the diffusion of N adatoms at the step edges.

Similar trends in the adsorption and desorption behavior of Ga and N adatoms on the surface with 1 ML excess Ga are found in the potential-energy profile of the stepped surface with 2 ML excess Ga. Fig. 7 shows the positions of Ga and N atoms and their potential-energy profiles along the [1 1 $\bar{0}$ 0] direction on the stepped surface with 2 ML excess Ga shown in Fig. 2(d). As shown in the potential-energy profile of the Ga adatom shown in Fig. 7(a), the most stable adsorption site is

located close to the step edges, but the adsorption energy near Step B ($E_{ad} = -2.80$ eV) is close to those in the other positions. The energy barrier for around the step edge is at most 0.74 eV, and the calculated ESB is -0.07 eV for Step A and -0.32 eV for Step B. The values of energy barriers for diffusion thus suggest that there is few specific energy barrier to overcome for diffusing up and down the step. The calculated attachment energies for the Ga adatom are -0.07 and -0.13 eV for Step A and Step B, respectively. The most stable adsorption site for the N adatom is located away from the step edges with $E_{ad} = -5.02$ eV, but the value is only 0.07 eV lower than those near the step edges. The small energy difference in the adsorption energy implies that the adsorption of N adatoms occurs not only near the step edge but also in the terrace region. The value of E_{ESB} estimated from the difference in barriers for step attachment between the upper and lower terraces is 0.28 (0.29) eV for Step A (Step B), which corresponds to the attachment energy. Therefore, the N adatom diffuses in both terrace and step edge regions with negligible ESB. Similar to the surface with 1 ML excess Ga, the N adatom is also stabilized with low adsorption energy (-5.35 eV) when it is located underneath the topmost Ga layer. It is also expected that the N adatom tends to diffuse into the bulk and affect the growth mode.

The calculated results on vicinal surfaces shown in Figs. 5–7 as well as the results on flat (0001) surfaces suggest that Ga adatoms diffuse much faster than N adatoms. Although this feature should be carefully examined by considering the the enhancement of N diffusion [36,38], we examine the Ga adatom diffusion on the stepped surfaces to understand the growth modes as follows. Fig. 8 illustrates the behavior of Ga adatoms on the stepped GaN(0001) surface along the [1 1 $\bar{0}$ 0] direction depending on the reconstruction. The adsorption energies at terraces in Fig. 8 are obtained from the (2×2) flat slab models. The ESB of Ga adatoms is present for the surface without Ga layer (Fig. 8(a)), while the ESB is negligibly small on the surface with 1 and 2 ML excess Ga (Figs. 8(b) and 8(c), respectively). The presence of ESB on the surface without excess Ga layers shown in Fig. 8(a) leads to the formation of islands near the edges of descending steps, consistent with the STM observation [14]. Furthermore, the absence of ESB and small diffusion barrier for the surface with 1 and 2 ML excess Ga shown in Figs. 8(b) and 8(c), respectively, suggests the inhibition of islands near the single layer steps. This trend has been actually observed by the STM for the surface with 1 and 2 ML excess Ga [14]. Furthermore, the absence of ESB implies that islands can be formed in the terrace region depending on the diffusion length. Although further studies to verify the presence or absence of ESB in the double layer steps depending on the reconstruction should be necessary, our calculations clarify the effect of ESB on the behavior of adatoms depending on the growth condition.

4. Summary

We have investigated the adsorption and desorption behavior of Ga and N atoms at step edges of GaN(0001) surface on the basis of *ab initio* calculations. We have found that the structure of single-layer step edges along the [1 1 $\bar{0}$ 0] direction depends on the growth condition. Furthermore, the adsorption behavior of Ga and N adatoms close to these step edges is found to be dependent on these structures. The Ga adatoms are preferentially incorporated at the step edge with low adsorption energy (-3.71 eV) and the ESB is recognized under moderately Ga-rich and N-rich conditions, while the ESB is negligibly small under Ga-rich condition. These results suggest that the nucleation preferentially occurs in the terrace under Ga-rich condition, reasonably consistent with the STM observation of GaN(0001) surface fabricated by the MBE.

Declaration of Competing Interest

The authors declare that they have no known competing financial interests or personal relationships that could have appeared to

influence the work reported in this paper.

References

[1] B. Heying, E.J. Tarsa, C.R. Elsass, P. Fini, S.P. DenBaars, J.S. Speck, J. Appl. Phys. 85 (1999) 6470.
[2] C. Adelmann, J. Brault, D. Jalabert, P. Gentile, H. Mariette, G. Mula, B. Daudin, J. Appl. Phys. 91 (2002) 9638.
[3] G. Koblmueller, J. Brown, R. Averbeck, H. Riechert, P. Pongratz, J.S. Speck, Jpn. J. Appl. Phys. 44 (2005) L906.
[4] A.L. Corrion, F. Wu, J.S. Speck, J. Appl. Phys. 112 (2012) 054903.
[5] N.A.K. Kaufmann, L. Lahourcade, B. Hourahine, D. Martin, N. Grandjean, J. Cryst. Growth 433 (2016) 36.
[6] I. Bryan, Z. Bryan, S. Mita, A. Rice, J. Tweedie, R. Collazo, Z. Sitar, J. Cryst. Growth 438 (2016) 81.
[7] K. Bellmann, U.W. Pohl, C. Kuhn, T. Wernicke, M. Kneissl, J. Cryst. Growth 478 (2017) 187.
[8] S. Vezian, F. Natali, F. Semond, J. Massies, Phys. Rev. B 69 (2004) 125329.
[9] G. Ehrlich, F.G. Hudda, J. Chem. Phys. 44 (1966) 1039.
[10] R.L. Schwoebel, E.J. Shipsey, J. Appl. Phys. 37 (1966) 3682.
[11] A. Pimpinelli, I. Elkinani, A. Karma, C. Misbah, J. Villain, J. Phys.-Condens. Matter 6 (1994) 2661.
[12] M.H. Xie, S.Y. Leung, S.Y. Tong, Surf. Sci. 515 (2002) L459.
[13] W. Hong, H.N. Lee, M. Yoon, H.M. Christen, D.H. Lowndes, Z.G. Suo, Z.Y. Zhang, Phys. Rev. Lett. 95 (2005) 4.
[14] H. Zheng, M.H. Xie, H.S. Wu, Q.K. Xue, Phys. Rev. B 77 (2008) 045303.
[15] Y. Kangawa, T. Akiyanama, T. Ito, K. Shiraishi, T. Nakayama, Materials 6 (2013) 3309.
[16] T. Akiyama, et al., Epitaxial Growth of III-Nitride Compounds, in: T. Matsuoka, Y. Kangawa (ed.), Springer, Berlin, 2018.
[17] J.P. Perdew, K. Burke, M. Ernzerhof, Phys. Rev. Lett. 77 (1996) 3865.
[18] N. Troullier, J.L. Martins, Phys. Rev. B 43 (1991) 1993.
[19] D. Vanderbilt, Phys. Rev. B 41 (1990) 7892.
[20] S.G. Louie, S. Froyen, M.L. Cohen, Phys. Rev. B 26 (1982) 1738.
[21] T. Akiyama, K. Nakamura, T. Ito, J.-H. Song, A.J. Freeman, Phys. Rev. B 80 (2009) 075316.
[22] J. Yamauchi, M. Tsukada, S. Watanabe, O. Sugino, Phys. Rev. B 54 (1996) 5586.
[23] H. Kageshima, K. Shiraishi, Phys. Rev. B 56 (1997) 14985.
[24] H.P. Maruska, J.J. Tietjen, Appl. Phys. Lett. 15 (1969) 327.
[25] J.E. Northrup, J. Neugebauer, R.M. Feenstra, A.R. Smith, Phys. Rev. B 61 (2000) 9932.
[26] Y. Yoshimoto, S. Tsuneyuki, Surf. Sci. 514 (2002) 200.
[27] J. Yamauchi, Y. Yoshimoto, Y. Suwa, Appl. Phys. Lett. 99 (2011) 191901.
[28] K. Shiraishi, J. Phys. Soc. Jpn. 59 (1990) 3455.
[29] M.D. Pashley, K.W. Haberern, W. Friday, J.M. Woodall, P.D. Kirchner, Phys. Rev. Lett. 60 (1988) 2176.
[30] J.E. Northrup, J. Neugebauer, R.M. Feensta, A.R. Smith, Phys. Rev. B 61 (2000) 9932.
[31] T. Ito, T. Nakamura, T. Akiyama, K. Nakamura, Appl. Surf. Sci. 254 (2008) 7659.
[32] T. Ito, T. Akiyama, K. Nakamura, J. Cryst. Growth 311 (2009) 698.
[33] T.K. Zywietz, J. Neugebauer, M. Scheffler, Appl. Phys. Lett. 73 (1998) 487.
[34] V. Jindal, F. Shahedipour-Sandvik, J. Appl. Phys. 105 (2009) 084902.
[35] T. Akiyama, K. Nakamura, T. Ito, Appl. Phys. Lett. 100 (2012) 251601.
[36] M. Chugh, M. Ranganathan, Phys. Chem. Chem. Phys. 19 (2017) 2111.
[37] Y. Kangawa, T. Ito, A. Taguchi, K. Shiraishi, T. Ohachi, Surf. Sci. 493 (2001) 178.
[38] J. Neugebauer, T.K. Zywietz, M. Scheffler, J.E. Northrup, H. Chen, R.M. Feenstra, Phys. Rev. Lett. 90 (2003) 056101.